Shadow Processing Method of High Resolution Remote Sensing Image Using IOBA Matching

Arya S Raj, Kavitha V K

P.G Scholar, Dept of CSE, BMCE, Kollam, Kerala, India

aryasraj13@gmail.com

Abstract— Shadows in remotely sensed images create difficulties in many applications; thus, they should be effectively detected prior to further processing. In accordance with the characteristics of high resolution color remote sensing images, we put forward a Shadow Processing Method of High Resolution Remote Sensing Image Using IOBA Matching with shape information preserved in color aerial images for solving problems caused by cast shadows. In this method, suspected shadows are extracted according to the statistical features of the images. Furthermore, some dark objects which could be mistaken for shadows are ruled out. Once the shadows are detected they are classified and a non-shadow area around each shadow termed as outer buffer area is estimated using IOBA matching. The mean and variance of these outer buffer areas are used to compensate the shadow regions. Experiments show that the new method can accurately detect shadows from urban high-resolution remote sensing images and can effectively restore shadows with a rate of over 85%.

Keywords — Shadow, Remote Sensing Image, Inner Buffer Area, Outer Buffer Area, IOBA matching, Shadow Detection, Shadow Removal.

INTRODUCTION

In the process of requirement of high resolution remote sensing image, shadows are casted by buildings especially present in urban environments. Shadows can be used to detect buildings and estimate the heights of the buildings [1]. But during the progress of remote sensing images, the shadows have adverse impact on the image. They cause loss of information for the surface under the shadows as well as difficulties for image interpretation, image matching, change detection and other applications. The motivation for this research is to remove the big shadow regions in images, so that objects covered by shadows can be easily extracted for applications.

Many effective algorithms have been proposed for shadow detection. Existing shadow detection methods can be roughly categorized into two groups [9,4]: model-based methods and shadow-feature-based methods. The first group uses prior information such as scene, moving targets, and camera altitude to construct shadow models [5], [6]. This group of methods is often used in some specific scene conditions such as aerial image analysis and video monitoring. The second group of methods identifies shadow areas with information such as gray scale, brightness, saturation, and texture.

An improved algorithm exists that combines the two methods [3]. First, the shadow areas are estimated according to the space coordinates of buildings calculated from digital surface models and the altitude and azimuth of the sun. Then, to accurately identify a shadow, the threshold value is obtained from the estimated grayscale value of the shadow areas. However, information such as scene and camera altitude is not usually readily available. Consequently, most shadow detection algorithms are based on shadow features. For example, the shadow region appears as a low grayscale value in the image, and the threshold is chosen between two peaks in the grayscale histogram of the image data to separate the shadow from the nonshadow region [2]. An illuminant invariance model has been used to detect shadows; this method can obtain a comparatively complete shadow outline from a complex scene and derive the shadow-free image by using certain neutral interface reflecting assumptions [7]. In a related study, images are converted into different invariant color spaces (HSV, HCV, YIQ, and YCbCr) to obtain shadows with Otsu's algorithm [8]. This can effectively get rid of the false shadows created by vegetation in certain invariant spaces. Based on that work, a successive thresholding scheme was proposed to detect shadows [9]. To avoid the false shadows of dark objects such as vegetation and moist soil, the normalized difference vegetation index [10], and the normalized saturation–value difference index area considered [11].

A variety of image enhancement methods have been proposed for shadow removal, such as histogram matching [2], gamma correction [13], linear correlation correction (LCC) [2], [13], and restoration of the color invariance model [8]. In a related study [13], several enhancement methods were analyzed to recover shadows, namely, gamma correction, LCC, and histogram matching. Inspired by this related analysis, a better approach was developed, based on a linear relationship between shadow classes and the corresponding

nonshadow classes [12]. In addition, a paired-region-based approach is employed to detect and remove the shadows in a single image by calculating the difference between the shadow and nonshadow regions of the same type [14]. Aside from the aforementioned methods, shadows can be retrieved using multisource data. For example, shadow pixels can be identified from the region of interest in an image and from another image obtained at a different time. Then, nonshadow pixels of the corresponding region are used to replace the shadow pixels. This latter approach is useful in low-resolution images [2].
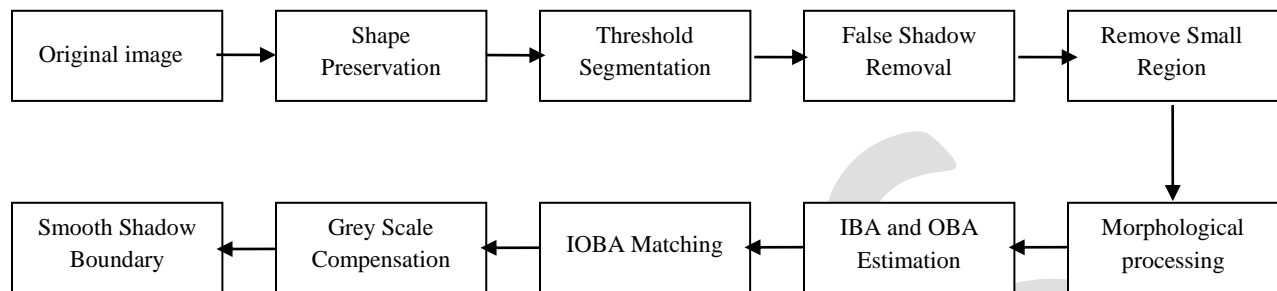

Fig.1 Flowchart of Shadow Processing Method of High Resolution Remote Sensing Image Using IOBA Matching

Due to the shortcomings of pixel-level shadow detection, in this study, we propose a new technique: a Shadow Processing Method of High Resolution Remote Sensing Image Using IOBA Matching. First, apply sobel operation for shape preservation, and then suspected shadows are detected with the threshold method of image segmentation. Next, the false shadows are ruled out (i.e., vegetation region). Then the shadow regions after removing the small regions are processed through mathematical morphology closed operation. This will allow only the real shadows to be detected in subsequent steps.

Shadow removal employs a series of steps. First we extract the inner and outer buffer area of each independent shadow region. Homogeneous sections are obtained through IOBA sectional matching. Finally, using the homogeneous sections, the mean and variance of the outer homogeneous sections is used to compensate the shadow region. The proposed method for shadow detection and removal is shown in Fig. 1.
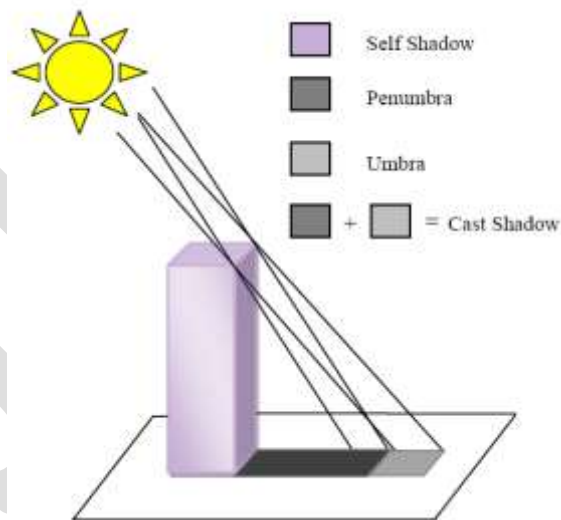

Fig. 2 Principle of shadow formation

PROPOSED METHOD

Shadows could be defined as the parts of the scene that is not directly illuminated by a light source due to an obstructing object or objects. A typical shadow could be divided into 2 different types. One type is denoted as self shadow where the shadow region is on the object itself. The other type is cast shadow for which the shadow region is on the background or on another objects. The cast shadow is usually further divided into 2 parts, umbra and penumbra. The umbra is created because the direct light has been completely blocked, while the penumbra is created by something partly blocking the direct light, as shown in Fig. 2. In remote sensing image we mainly focus only on the shadows in the cast shadow area. The proposed method consists of the following steps:

A. Shape Preservation

The shape preservation process is an option for providing additional shape information of the shadow-casting cultural features. The component is used in finding the boundaries and shapes of cultural features and dark regions, including shadows in which luminance is obstructed. A Sobel operator is applied on the gray component for shape preserved threshold segmentation,

B. Threshold Segmentation

For shadow detection, a properly set threshold can separate image into non-shadowed regions and shadow regions without too many pixels being misclassified [2]. Researchers have used several different methods to find the threshold to accurately separate shadow and non-shadow areas. Bimodal histogram splitting provides a feasible way to find the threshold for shadow detection, and the mean of the two peaks is adopted as the threshold [2]. Attain the threshold according to the histogram of the original image and then find the suspected shadow objects by comparing the threshold and grayscale average of each object obtained in segmentation. Chose the grayscale value with the minimum frequency in the neighborhood of the mean of the two peaks as the threshold, as shown in

$$G_q = \frac{1}{2}(G_m + G_s) \tag{1}$$

$$h(T) = Min\{h(G_q - \varepsilon), h(G_q + \varepsilon)\} \tag{2}$$

In the equations, G_m is the average grayscale value of an image; G_s stands for the left peak of the shadow in the histogram; T is the threshold; ε represents the neighborhood of T, where T ∈ $[G_q - \varepsilon, G_q + \varepsilon]$; and h(I) is the frequency of I, where I = 0, 1, . . . , 255. To avoid the influence of abnormal information, 2% of the pixels on the left and right sides of the histogram are not included.

C. False Shadow Removal

Dark objects may be included in the suspected shadows, so more accurate shadow detection results are needed to eliminate these dark objects. Rayleigh scattering results in a smaller grayscale difference between a shadow area and a non-shadow area in the blue (B) waveband than in the red (R) and green (G) wavebands. Consequently, for the majority of shadows, the grayscale average at the blue waveband G_b is slightly larger than the grayscale average at the green waveband G_g. Also, the properties of green vegetation itself make G_g significantly larger than G_b, so false shadows from vegetation can be ruled out by comparing the G_b and G_g of all *suspected* shadows.

D. Remove Small Region

After initial image segmentation, an area of every independent decomposed region is computed. If it is lower than threshold value, it can be considered as surface features with low-light level in non-shadowed region and it is ruled out from shadow region.

E. Morphological processing

But in this case, cavity may appear because of extensive surface features with high-light level within shadow regions. Shadow regions after segmentation are processed through mathematical morphology closed operation.

F. IBA and OBA Estimation

Outer Buffer area (OBA) of each shadow region is the non shadow area around that connected shadow component. Thus, after determining the connected component, the Inner and Outer Buffer Area of each connected shadow components is computed using morphological dilation or erosion operation and image subtraction operation as follows:

$$I_{dilated,k} = (I_k \oplus B_{square}) \tag{3}$$

$$I_{eroded,k} = (I_k \oplus B_{square}) \tag{4}$$

The dilation operation will expand the shadow boundaries and the erosion operation will contract the shadow boundaries. B_{square} is a square structuring element. The size of the structuring element will decide the size of Inner and Outer Buffer Area. In this paper a 3x3 square structuring element is used.

$$I_{OBA,k} = (I_{dilated,k} - I_k) \tag{5}$$

$$I_{IBA,k} = (I_{dilated,k} - I_k) \tag{6}$$

where k = 1,2,....m and m represent the sets of connected components or m different shadows in the image. m can have the value one or greater than one , depending on the number of shadows..

G. IOBA Matching

To recover the shadow areas in an image, we use a shadow removal method based on IOBA matching. There is a large probability that both shadow and non-shadow areas in close range on both sides of the shadow boundary belong to the same type of object. The Buffer Area (BA) in the shadow area is marked as Inner Buffer Area (IBA); Buffer Area (BA) in the non-shadow area is marked as Outer Buffer Area (OBA). When the correlation between IBA and OBA is close enough, there is a large probability that this location belongs to the same type of object. That is, similarity matching needs to be applied to the inner and outer buffer area section by section to rule out the two kinds of non-homogeneous sections.

To rule out the non-homogeneous sections, the inner and outer buffer area is divided into average sections with the same standard, and then, the similarity of each buffer area is calculated section by section. If the variance between inner and outer buffer area at a section is small, it means that the shade and light fluctuation features of the buffer area pair at this section are consistent. If consistent, then this buffer area pair belongs to the same type of object, with different illuminations, and thus is considered to be matching. If the variance between inner and outer buffer area at a section is large, then some abnormal parts representing some different types of objects exist in this section; therefore, there outer buffer area parts should be ruled out, as shown in Fig. 3.
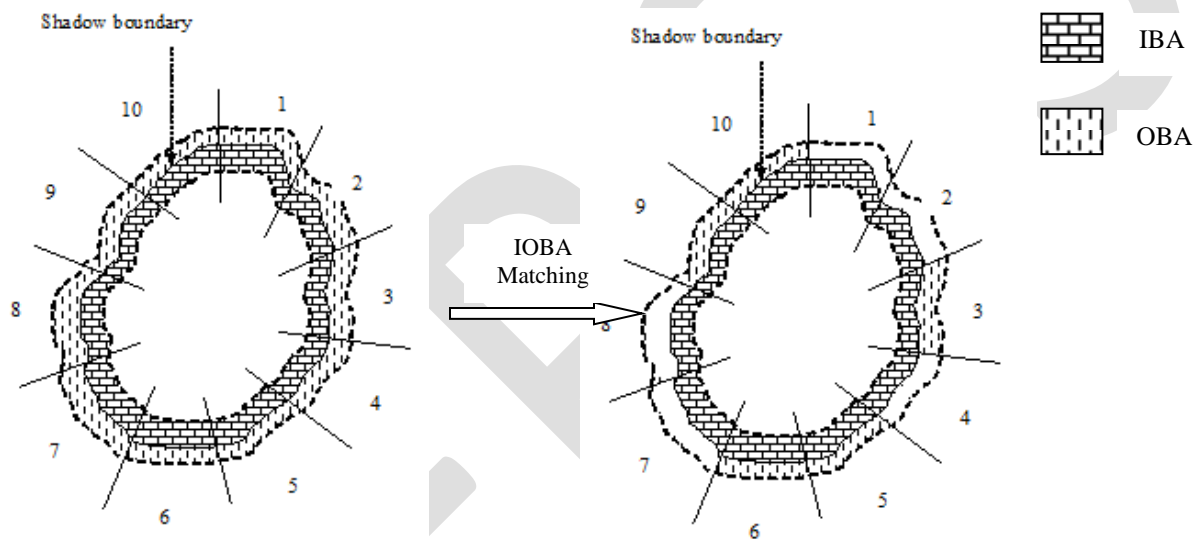

Fig. 3 Diagram of IOBA matching

H. Grey Scale Compensation

Shadows are removed, with the homogeneous sections (section - 3, 4, 5, 6, 9, 10) obtained by IOBA matching, using the following transformation function. That is, the mean and variance of outer buffer area after IOBA matching and mean and variance of shadow region is used to compensate the shadow region.

$$I'_k = \mu_{OBA',k} + \frac{I_k - \mu_k}{\sigma_k} * \sigma_{OBA',k} \qquad (7)$$

where k = 1,2,....m . I'_k is the compensated value of the shadow pixel. $\mu_{OBA',k}$ and $\sigma_{OBA',k}$ are the mean and variance of the outer buffer area after IOBA matching. μ_k and σ_k the mean and variance of the corresponding shadow region. The resulting image is shadow free image.

I. Smooth Shadow Boundary

After processing mentioned above, an obvious boundary-line appears between shadow regions and clear surface feature regions. Fig. 4 can explain the reason of this phenomenon. Fig. 4 left is a typical boundary-line, vertical line means shadow regions boundary. Fig. 4 the right one is shadow boundary after processing. It is observed that a sudden gray change due to transition zone appears on shadow boundary. This is a strong boundary effect. To reduce this effect, a median filtering along shadow boundary could be in progress after grey scale compensation, so that transition of shadow regions to non-shadowed regions could be in progress.
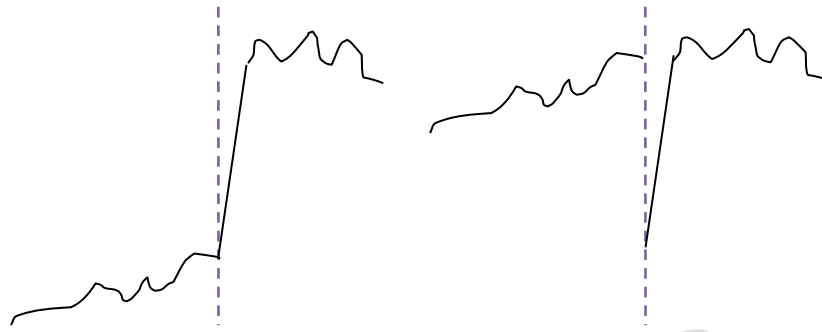
Fig. 4 Boundary regions before and after grey scale compensation

EXPERIMENTAL RESULTS

In order to test the validity of this method, a remote sensing image is used. Fig.3 shows the results of our proposed system. The accuracy of shadow detection can be seen from the fact that roads and vegetation regions are not detected as shadows, though they have similar characteristics as shadows. In the process of shadow removal on the high resolution remote sensing image, information in shadow regions should be tried to restore while information in non-shadowed regions should be tried to reserve.
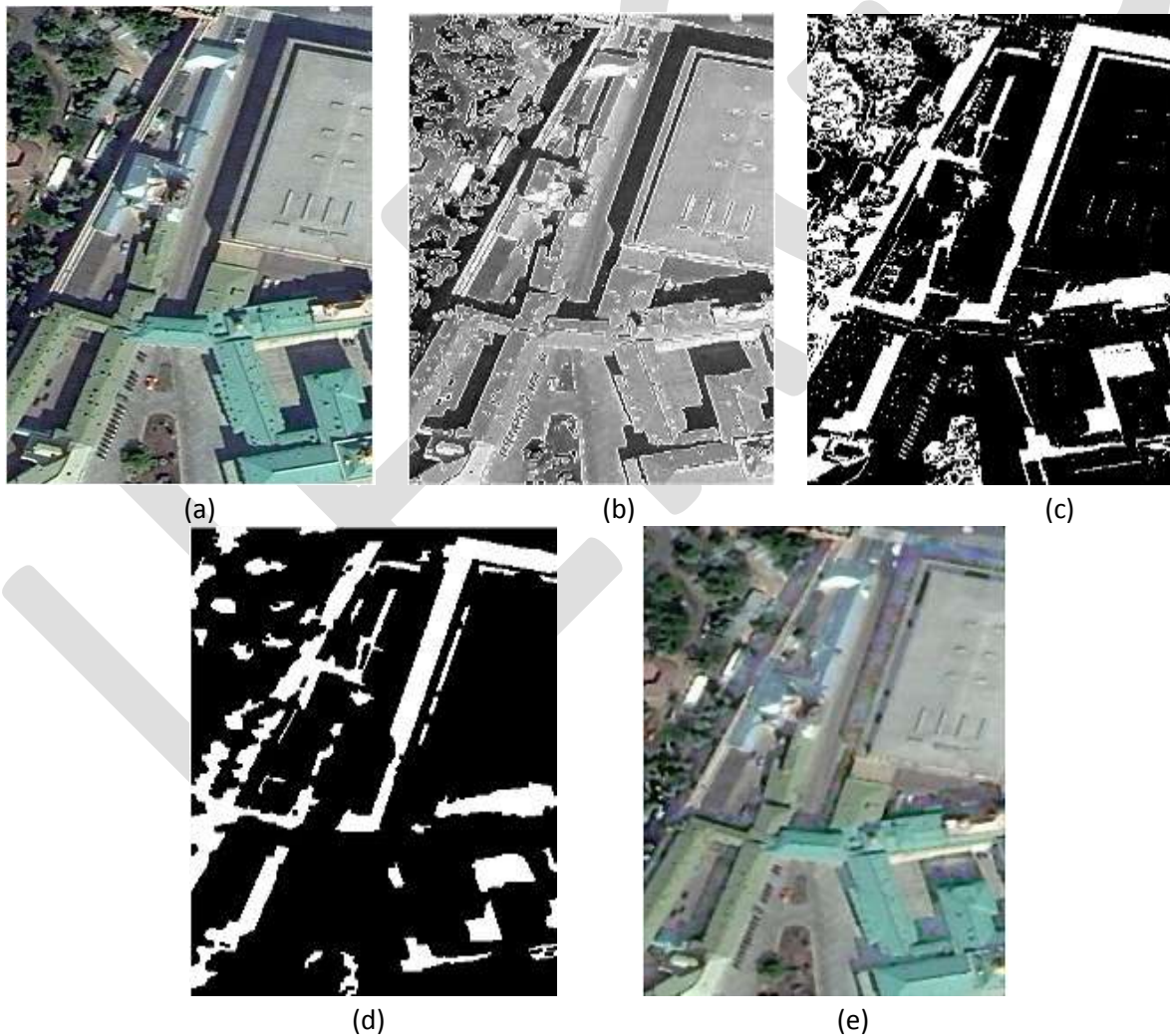

(a) (b) (c)

(d) (e)

Fig.3 The results of proposed system (a) Original Image (b) Segmentation Result (c) Result of Shadow Detection (d) Result of Shadow Detection after False Shadow Removal (e) Recovered Image

CONCLUSION

This paper put forward a systematic and effective method for shadow detection and removal in a single high-resolution remote sensing image. In order to get a shadow detection result, image segmentation considering shadows is applied first. It classifies shadow and non-shadow region using threshold segmentation and false shadows are ruled out. After the homogeneous sections are obtained using IOBA matching, the mean and variance value of the outer buffer area around each shadow region is used to compensate the shadow region.

REFERENCES:

[1] T. Kim, T. Javzandulam, and T.-Y. Lee, "Semiautomatic reconstruction of building height and footprints from single satellite images," in *Proc. IGARSS*, Jul. 2007, vol. 2, pp. 4737–4740.

[2] P.M. Dare, "Shadow analysis in high-resolution satellite imagery of urban areas," *Photogramm. Eng. Remote Sens.*, vol. 71, no. 2, pp. 169–177, 2005.

[3] Y. Li, P. Gong, and T. Sasagawa, "Integrated shadow removal based on photogrammetry and image analysis," *Int. J. Remote Sens.*, vol. 26, no. 18, pp. 3911–3929, 2005.

[4] J. Yoon, C. Koch, and T. J. Ellis, "ShadowFlash: An approach for shadow removal in an active illumination environment," in *Proc. 13th BMVC*, Cardiff, U.K., Sep. 2–5, 2002, pp. 636–645.

[5] R. B. Irvin and D. M. McKeown, Jr, "Methods for exploiting the relationship between buildings and their shadows in aerial imagery," *IEEE Trans. Syst., Man, Cybern.*, vol. 19, no. 6, pp. 1564–1575, Dec. 1989.

[6] Y. Li, T. Sasagawa, and P. Gong, "A system of the shadow detection and shadow removal for high resolution city aerial photo," in *Proc. ISPRS Congr, Comm.*, 2004, vol. 35, pp. 802–807, Part B3.

[7] E. Salvador, A. Cavallaro, and T. Ebrahimi, "Shadow identification and classification using invariant color models," in *Proc. IEEE Int. Conf. Acoust., Speech, Signal Process.*, 2001, vol. 3, pp. 1545–1548.

[8] V. J. D. Tsai, "A comparative study on shadow compensation of color aerial images in invariant color models," IEEE Trans. Geosci. Remote Sens., vol. 44, no. 6, pp. 1661–1671, Jun. 2006.

[9] K.-L. Chung, Y.-R. Lin, and Y.-H. Huang, "Efficient shadow detection of color aerial images based on successive thresholding scheme," *IEEE Trans. Geosci. Remote Sens.*, vol. 47, no. 2, pp. 671–682, Feb. 2009.

[10] D. Cai, M. Li, Z. Bao *et al.*, "Study on shadow detection method on high resolution remote sensing image based on HIS space transformation and NDVI index," in *Proc. 18th Int. Conf. Geoinformat.*, Jun. 2010, pp. 1–4.

[11] [15] H. Ma, Q. Qin, and X. Shen, "Shadow segmentation and compensation in high resolution satellite images," in *Proc. IEEE IGARSS*, Jul. 2008, vol. 2, pp. 1036–1039.

[12] L. Lorenzi, F. Melgani, and G. Mercier, "A complete processing chain for shadow detection and reconstruction in VHR images," *IEEE Trans. Geosci. Remote Sens.*, vol. 50, no. 9, pp. 3440–3452, 2012.

[13] P. Sarabandi, F. Yamazaki, M. Matsuoka *et al.*, "Shadow detection and radiometric restoration in satellite high resolution images," in *Proc. IEEE IGARSS*, Sep. 2004, vol. 6, pp. 3744–3747.

[14] R. Guo, Q. Dai, and D. Hoiem, "Single-image shadow detection and removal using paired regions," in *Proc. IEEE Conf. Comput. Vis. Pattern Recog.*, 2011, pp. 2033–2040.

[15] Zhouwei Zhang and Fen Chen "A Shadow Processing Method of High Spatial Resolution Remote Sensing Image" 3rd International Congress on Image and Signal Processing, 2010

[16] Krishna Kant Singh, Kirat Pal and M.J.Nigam, "Shadow Detection and Removal from Remote Sensing Images Using NDI and Morphological Operators," International Journal of Computer Applications (0975 – 8887) Volume 42– No.10, March 2012.